

Multidimensional paperfolding systems

Shelomo I. Ben-Abraham,^{a*} Alexander Quandt^b and Dekel Shapira^{a‡}^aDepartment of Physics, Ben-Gurion University of the Negev, IL-84105 Beer-Sheva, Israel, and^bSchool of Physics and DST/NRF Centre of Excellence in Strong Materials, University of the Witwatersrand, Private Bag 3, Wits, 2050, Johannesburg, South Africa. Correspondence e-mail: benabr@bgu.ac.il

Algorithms for constructing aperiodic structures produce templates for the nanofabrication of arrays for applications in photonics, phononics and plasmonics. Here a general multidimensional recursion rule is presented for the regular paperfolding structure by straightforward generalization of the one-dimensional rule. As an illustrative example the two-dimensional version of the paperfolding structure is explicitly constructed, its symbolic complexity referred to rectangles computed and its Fourier transform shown. The paperfolding structures readily yield novel ‘paperfolding’ tilings. Explicit formulas are put forward to count the number of folds in any dimension. Finally, possible generalizations of the dragon curve are discussed.

© 2013 International Union of Crystallography
Printed in Singapore – all rights reserved

1. Introduction

The purpose of this paper is to present a simple, clear, transparent algorithm for creating an unprecedented two- or three-dimensional structure as a template for its physical realization as well as the necessary basic information about it. It is written by physicists and intended for nanoscientists, crystallographers, electron microscopists and condensed matter physicists in general. Dimensions beyond three are simply a concomitant bonus. Nevertheless, we would be pleased if expert mathematicians and computer science theorists should meet the challenge and elaborate the subject in a rigorous formal manner.

To the best of our knowledge, the paperfolding (PF) sequence and the closely related dragon curve were first invented (or discovered?), at least in the West, by three physicists: John E. Heighway, Bruce A. Banks and William G. Harter. The sequence and the curve were publicized in 1967 by the great Martin Gardner in his legendary column ‘Mathematical Games’, which quite often spawned serious and important research (Gardner, 1967*a,b,c*). Somewhat later Chandler Davis and Donald Knuth thoroughly elaborated the subject (Davis & Knuth, 1970*a,b*).

Since then the regular paperfolding (RPF) sequence has become one of the standard, if not to say paradigmatic, aperiodic systems. A comprehensive and readable account was published in the *Mathematical Intelligencer* (Dekking *et al.*, 1982*a,b,c*). Newer references are the seminal book by Allouche & Shallit (2003) and a recent paper by Dekking (2012).

Almost all of the literature about paperfolding sequences is limited to one dimension. A notable exception is ‘*Quelles*

tuiles!’ by Salon (1989), a most interesting and important paper. Most regrettably it went largely unnoticed. After we submitted this paper one of the referees drew our attention to it. Salon discovered that the edges of the Robinson tiling (Robinson, 1971; Grünbaum & Shephard, 1986) form a two-dimensional paperfolding structure. He then found that the structure can be physically realized by folding a handkerchief. We went the other way. We started by folding a sheet of paper first from left to right and then from bottom to top and looked for an algorithm that reproduces the result.

For physical applications it is interesting to construct multidimensional analogues of the PF sequence. Two- and three-dimensional versions of aperiodic sequences serve as templates to fabricate photonic, phononic and plasmonic structures, such as virtually isotropic bandpass filters and particularly patterns for ‘light in tiny holes’ (EOT – extraordinary optical transmission of light through patterned arrays of subwavelength orifices) (*cf.* Genet & Ebbesen, 2007). Recently we have constructed a two-dimensional paperfolding (2D PF) structure and computed its line complexity using a simplified version (Ben-Abraham & Quandt, 2011) of a recursive algorithm suggested by Barbé & von Haeseler (2004, 2005, 2007). It turned out that the algorithm causes the structure to be extremely fractal, consisting of widely scattered islands, which is useless for applications and rather inconvenient for presentation. In Fig. 1 we show the ninth generation of the recursion. With some serious numerical effort we were actually able to generate structures which correspond to up to 13 recursions. But the final patterns are so scattered that one can hardly see anything. This was a strong motivation for us to find an alternative approach based on actual paper folding. We eventually succeeded in deriving a straightforward generalization of the one-dimensional recursion rule.

‡ Present address: The Racah Institute of Physics, The Hebrew University, IL-91904 Jerusalem, Israel.

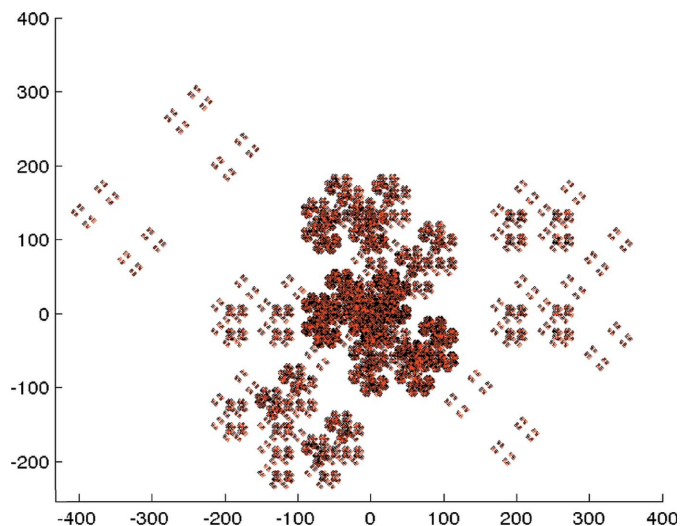


Figure 1
Ninth generation of two-dimensional PF constructed by the simplified Barbé-von Haeseler recursion.

2. Preliminary observations

The RPF sequence is usually defined as follows. Let $A_2 = \{a, b\}$ be the alphabet of symbols, $S(n)$ the chain after n iterations and m' the operator of reversing a word and interchanging the symbols. The notation m' is taken from crystallography where it signifies a mirror with colour interchange. In the present case it reverses the string and interchanges the symbols. That operation will be useful in what follows. Using the conventions mentioned above the recursion rule becomes

$$\begin{aligned} S(n + 1) &= S(n) a m' S(n), \\ S(1) &= a. \end{aligned} \tag{1}$$

The first three generations thus become

$$\begin{aligned} &a \\ &aab \\ &aabaabb \end{aligned} \tag{2}$$

The conventional PF sequences are considered as one sided and defined on the natural numbers \mathbb{N} . The leftmost entry is always the image of the number 1. In Ben-Abraham & Quandt (2011) we constructed a double-sided version defined on the set of all integers \mathbb{Z} by concatenating to the left the sequence's antipalindrome. One of the referees pointed out that the PF sequence is by itself already double sided. That is true provided that the pivot a is invariably fixed on zero and thus the left half-chain sits on the negative integers.

In 'reality' one folds a (quasi) two-dimensional sheet of paper, and in contrast to conventional paper folding as a tangible realization of the sequences, which are one dimensional, the folds are zero-dimensional points. Yet another, transversal, dimension is necessary to perform the folding, to wit, the perpendicular to the sheet of paper. It leaves its trace as the sign of the entries, 'valley' (a or $+$) or 'crest' (b or $-$). It reappears and fully manifests itself after unfolding to produce a dragon curve.

In a natural way, most people are inclined to fold from right to left resulting in the recursion (1). However, it turns out that this is somewhat inconvenient for generalizations. Therefore we shall change the convention such that at step $(n + 1)$ of the iteration the n th patch $S(n)$ will always be in the all $+$ sector and the 'pivot' $S(1) = a$ (or the centre of its analogue) will always be at the origin.

3. The recursion

Bearing in mind RPF structures in arbitrary dimensions, let us suggest some conventions. Referring to Cartesian axes x_k ($k = 1, \dots, d$) we always fold from the negative to the positive half axis and cycle from 1 to d . Thus, for instance, in three dimensions the folding cycle becomes

$$\text{left} \rightarrow \text{right}, \text{bottom} \rightarrow \text{top}, \text{back} \rightarrow \text{front}. \tag{3}$$

Without losing generality we shall use the alphabet $A_2 = \{+, -\}$ ($+$ for 'valley', $-$ for 'crest'). Thus, in one dimension we define the RPF sequence by the recursion rule

$$\begin{aligned} S(n + 1) &= m' S(n) + S(n), \\ S(0) &= \emptyset. \end{aligned} \tag{4}$$

Here \emptyset denotes the empty chain.

In two dimensions the recursion rule becomes

$$\begin{aligned} &+ \\ &m'_1 S(n) : S(n) \\ &+ \\ S(n + 1) &= - \dots - - \dots + + \dots + \\ &+ \\ &m'_2 m'_1 S(n) : m'_2 S(n) \\ &+ \end{aligned} \tag{5}$$

Here m'_k denotes a mirror perpendicular to the axis k with colour change; in other words, reversing the string and interchanging the symbols. The first left-to-right fold, *i.e.* the vertical one, consists of a valley only, denoted here by $+$. The following bottom-to-top fold has all valleys ($+$) at its right half and all crests ($-$) at its left half.

In two dimensions the following identities are valid:

$$m'_2 m'_1 \equiv m_2 m_1 \equiv 2 \equiv \bar{1}, \tag{6}$$

that is, the two colour mirrors result in a rotation by 180° , which in two dimensions is the same as inversion. In higher dimensions additional specifications are necessary.

In two dimensions, the folds are straight line segments. In the more general case of d dimensions, they are $(d - 1)$ -dimensional facets.

Henceforth, the seed or fundamental motif $S(1)$ in any dimension d will be called the 'pivot'. In one dimension it is simply a point dividing the line into two half-lines, in two dimensions a cross, *i.e.* the inner edges of the four square cells around the origin, in three dimensions the inner faces of the

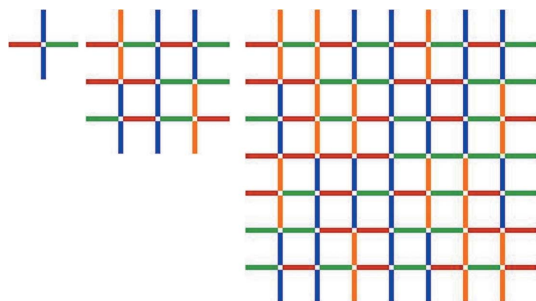


Figure 2
The first three generations of two-dimensional RPF constructed by recursion.

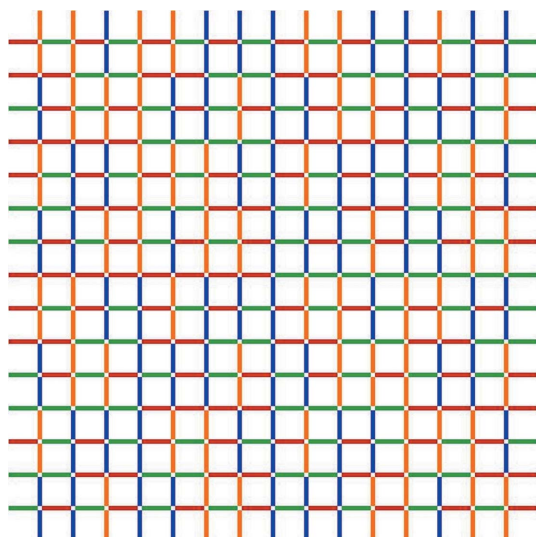


Figure 3
The fourth generation of two-dimensional RPF constructed by recursion.

eight cubic cells around the origin, and analogously in higher dimensions.

It is advantageous to switch from the two-letter alphabet $A_2 = \{+, -\}$ to the four-letter alphabet $A_4 = \{|| - -\}$. This allows one to distinguish between horizontal and vertical folds. Moreover, it immediately generalizes to any dimension. Thus there are always two variants of the structure: a *full* (or *coloured*) variant with $2d$ (colour) symbols and a *reduced* (or *black-and-white*) variant with only two symbols $+$ and $-$. Fig. 5 shows the fourth generation of the reduced variant. This should be compared with Fig. 3 which shows the corresponding full variant.

For convenience we use the following colour code. The ‘valleys’ perpendicular to the horizontal x axis are coloured by the shortest wavelength, say violet in three dimensions, those perpendicular to y by blue and those perpendicular to z by green. The ‘crests’ get the complementary colours: yellow, orange and red, respectively. And of course, analogically in any dimension.

Fig. 2 shows the three first generations of the two-dimensional RPF structure. Figs. 3 and 4 show the fourth and sixth generations, respectively. By now we have proceeded up

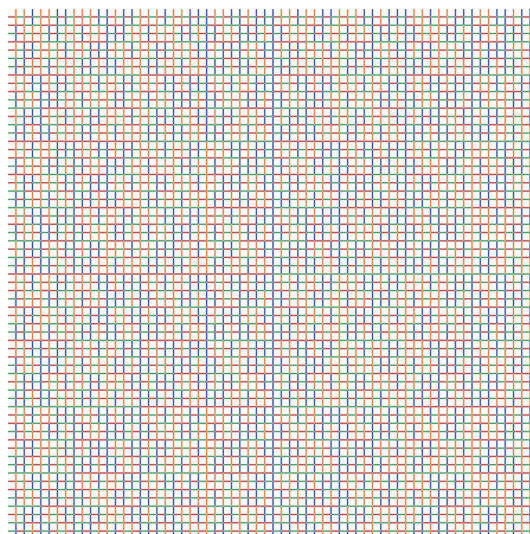


Figure 4
The sixth generation of two-dimensional RPF constructed by recursion.

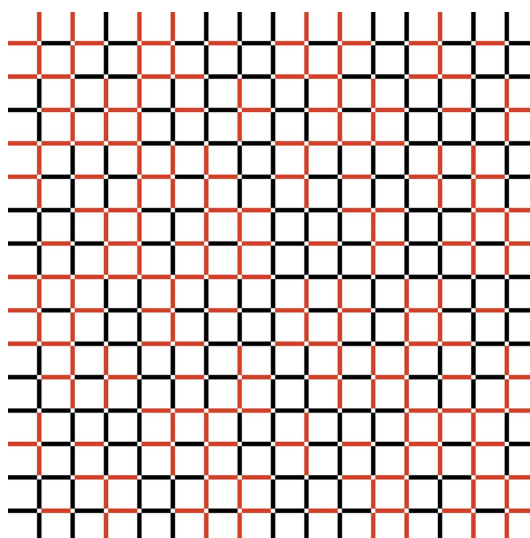


Figure 5
Reduced variant of fourth generation of two-dimensional RPF, to be compared with Fig. 3.

to the ninth generation and we still continue, mainly in order to further investigate the rectangle complexity. However, to show a printed picture, more recursions might be more confusing than illuminating.

As an illustration of ‘paperfolding’ in higher dimensions, Fig. 6 shows the first and second generation of the three-dimensional PF structure. Detailed elaboration of the three-dimensional and four-dimensional structures is in progress.

4. ‘Paperfolding’ tilings

PF structures can be readily turned into tilings (PFTs). That holds for general PF structures, that is, not necessarily regular ones.

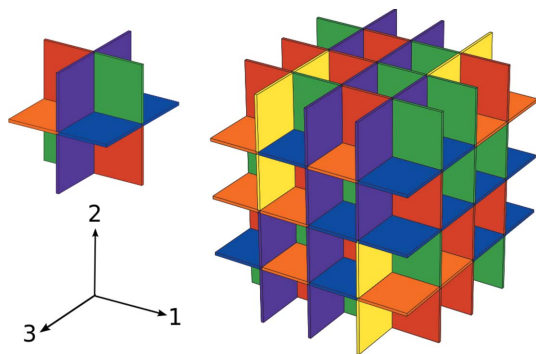


Figure 6
The first and second generations of the three-dimensional PF structure.

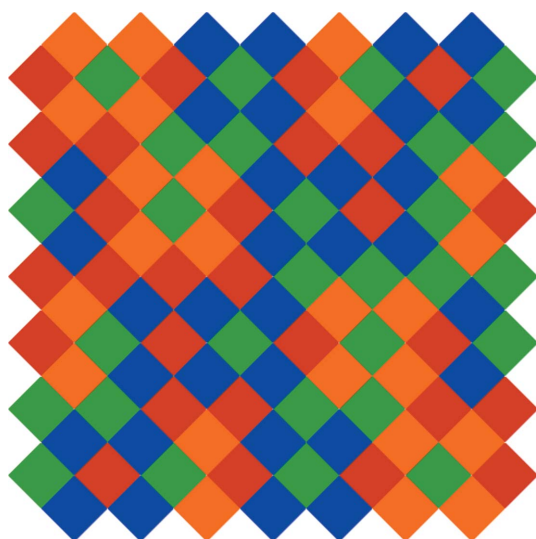


Figure 7
The third generation of the two-dimensional 'paperfolding' tiling.

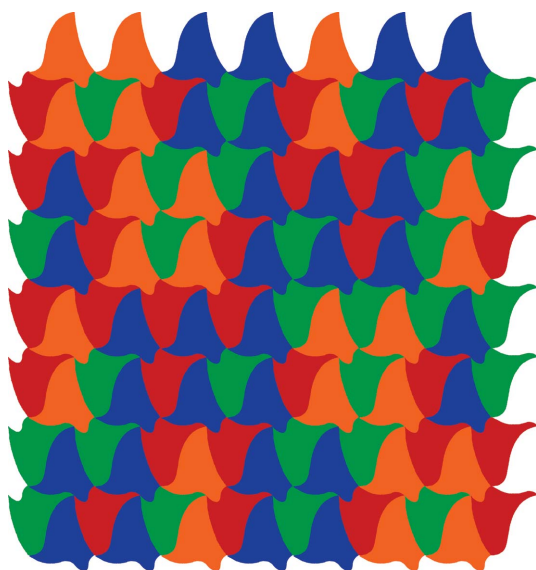


Figure 8
The third generation of a two-dimensional deformed 'paperfolding' tiling.

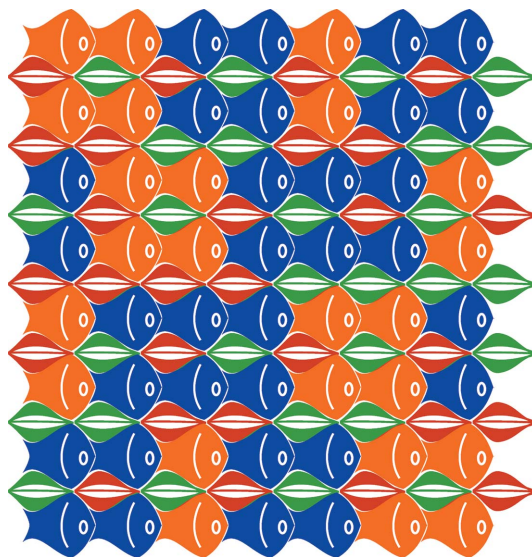


Figure 9
The third generation of a two-dimensional 'paperfolding' tiling *à la* Escher.

To turn a PF into a PFT all that is needed is to put points at the cell centres and connect them to the cell vertices. This creates cross polytopes with the folds as their equatorial (hyper-)planes. The vertices and the centres of the cell will be the vertices of the tilings. Thus, for instance, in one dimension we get line segments centred on the fold points, in two dimensions we get squares at 45° to the cells with the folds as one of their diagonals.

The one-dimensional case is quite trivial, but in two and higher dimensions the tilings become interesting. Fig. 7 shows the third generation of the two-dimensional tiling. For clarity we do not show higher generations.

By displacing the vertices of the tiling within the cells we can create tilings with tiles different from regular cross-polytopes. When the displacements are the same in all cells we simply change the tiles into identical deformed polytopes. However, we may displace the tiling vertices differently in different cells. That may be done by some deterministic rule but at random as well. We may even change the polytopes' edges into curved segments. Topologically all that does not change anything but geometrically we get an uncountable infinity of tiling variants. Fig. 8 shows such an arbitrarily deformed tiling. Fig. 9 shows a 'fish and mussels' tiling *à la* Maurice Escher.

5. Complexity matrix

To start with, a few preliminary definitions are in order, for the benefit of the general readership. *Symbolic complexity* $p_S(w|N)$ is the number of different words (configurations) w of size N in a given structure S . *Line complexity* $p_S(w|n)$ is symbolic complexity referred to a one-dimensional subset of a structure. For instance, if the structure is supported by a two-dimensional square lattice it is the complexity of rows and columns, and it is then called *row complexity* and *column*

Table 1
Rectangle complexity $p(N)$ related to A_4 .

N	1	2	3	4	5	6	7	8	9	10	11	12	13	14
p	4	16	32	88	84	320	176	548	468	844	410	1656	542	1396
N	15	16	17	18	19	20	21	22	23	24	25	26	27	28
p	1396	2020	808	2904	984	3300	2244	2700	1320	5500	1200	2476	2196	4044

Table 2
Complexity matrix $p(m, n)$ related to A_4 .

m	$n = 1$	2	3	4	5	6	7	8	9	10	11	12	13	14	15	16	17	18	19	20	21	22	23	24
1	4	8	16	24	36	48	64	76	96	116	136	156	184	212	252	288	324	624	360	396	432	468	504	540
2	8	32	112	192	304	408	512	608	736	864														
3	16	80	192	288	408	540																		
4	32	136	256	368	512																			
5	48	192	316	440	608																			
6	80	232	368	504																				
7	112	272	420	564																				
8	144	312	472																					
9	180	360	540																					
10	232	416																						
11	274	472																						
12	316	528																						
13	358	584																						
14	400	620																						
15	440																							
16	480																							
17	520																							
18	576																							
19	624																							
20	672																							
21	720																							
22	768																							
23	816																							
24	864																							

complexity, respectively. Rectangle complexity $p_S(w|m \times n)$ is the symbolic complexity of a structure supported by a two-dimensional square lattice considering rectangles of size $N = m \times n$ as the relevant configurations.

For the one-dimensional PF sequences the symbolic complexity is known to be $p_{PF}(n) = 4n$ for all $n \geq 7$ (Allouche,

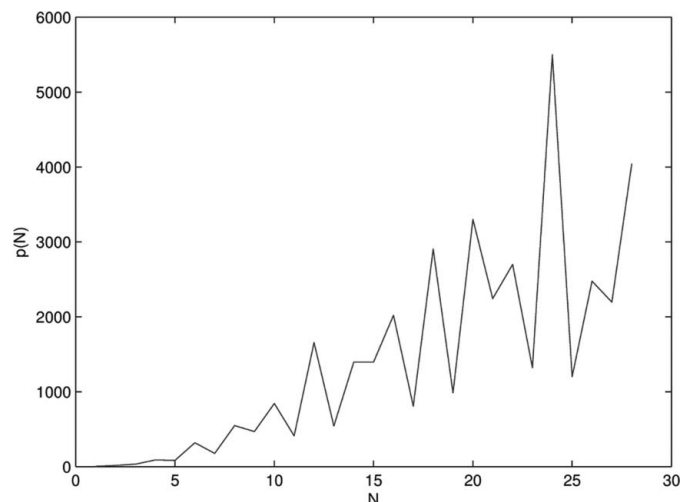


Figure 10
Rectangle complexity $p(N)$ related to A_4 .

1992). Alas, for higher dimensions there are no known formulas. The most that is known is that asymptotically the complexity behaves like N^d (Julien, 2009, 2010).

As can be seen from Table 1 and Fig. 10, the rectangle complexity $p(N)$ referred to the area $N = m \times n$ of the $m \times n$ rectangles oscillates wildly. These oscillations are a misleading artefact due to the factorization of N . For instance, $p(N)$ always sharply drops when N is a prime number. Therefore, rather than presenting $p(N)$ as a one-dimensional sequence, we shall present $p(m, n)$ as an infinite matrix (Table 2). Then the line entries (rows and columns) increase monotonically. However, since the computation is limited to some maximal N , only the upper left corner of $p(m, n)$ will be occupied. Analogously, in a higher dimension d the complexity becomes a d -dimensional array $p(m_1, \dots, m_d)$.

We computed the rectangle complexity up to $N = 30$, but we present only those results whose convergence was checked through three consecutive generations.

6. The count

It is interesting to determine how many folds there are in a given generation $S(n)$ of the structure. We denote this number by $|S(n)|$.

In d dimensions the number of sectors (half-axes, quadrants, octants, n -ants) is

$$\begin{aligned} \#(\text{sectors}) &= \#(\text{vertices of } d\text{-cube}) \\ &= \#(\text{facets of } d\text{-cross}) = 2^d. \end{aligned} \quad (7)$$

The number of folds in the ‘pivot’, that is, all mirrors, is

$$\begin{aligned} \#(\text{pivot}) &= \#(\text{mirrors}) \times \#(\text{folds in mirror}) \\ &= 2^{d-1} \times 2^{(d-1)n} d, \end{aligned} \quad (8)$$

where

$$\begin{aligned} \#(\text{mirrors}) &= \left[\frac{1}{2} \#(\text{sectors}) \right] \times \left[\frac{1}{2} \#(\text{faces of } d\text{-cube}) \right] \\ &= 2^d \times 2d/4 = 2^{(d-1)} d \end{aligned} \quad (9)$$

and

$$\#(\text{folds in mirror}) = 2^{(d-1)n}. \quad (10)$$

The latter follows from equation (7) by the following geometrical reasoning. Consider a coordinate axis and the $(d - 1)$ -dimensional plane perpendicular to it through the origin. That plane contains some of the facets of the sectors located around the origin, *i.e.* some of the mirrors needed to generate the PF structure in d dimensions. Furthermore, the plane cuts the sectors in two equal pieces and therefore the number of facets in that plane will be $2^d/2 = 2^{d-1}$.

Again, by construction, those facets will act as mirrors in our generalization of the PF sequence in d dimensions. Application of our general prescription to generate a PF structure in d dimensions will then transport all the mirrors of this first generation into the starting sector, where they are subject to the various mirror operations described above. If we now look at the necessary pivot(s) along the plane perpendicular to the chosen coordinate axis, we realize that the number of mirrors must grow by a factor of 2^{d-1} to match the size of the various new motifs generated by the mirror operations.

The same reasoning applies to all the other mirrors perpendicular to the various coordinate axes, and after n applications of the basic recursion step in d dimensions, the size of a new generation of mirrors substituting each mirror of a previous generation is given exactly by equation (10).

Therefore the generalization of the PF sequence in d dimensions leads to the following recursion formula:

$$\begin{aligned} |S(n+1)| &= \#(\text{sectors})|S(n)| + \#(\text{pivot}) \\ &= 2^d |S(n)| + 2^{d-1} \times 2^{(d-1)n} d \\ &= 2^d |S(n)| + 2^{(d-1)(n+1)} d, \\ |S(0)| &= 0. \end{aligned} \quad (11)$$

This also yields a closed formula for any dimension d and generation n :

$$|S(n)| = 2^{(d-1)n} (2^n - 1) d, \quad d, n \in \mathbb{N}_0. \quad (12)$$

The proof is by straightforward induction.

Specifically we have

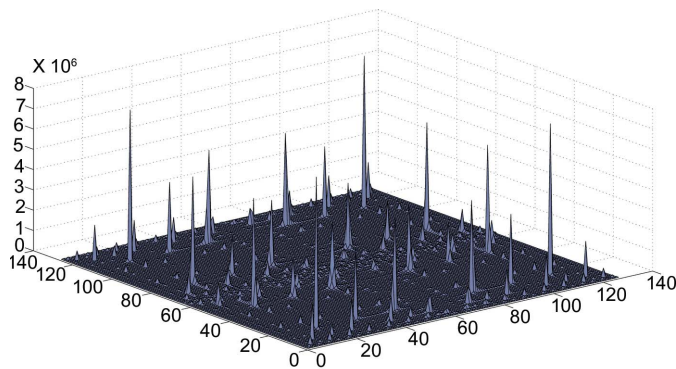


Figure 11
Fourier transform of the sixth generation of two-dimensional RPF.

$$\begin{aligned} 1\text{D} : |S(n)| &= 1 \times 2^{0n} (2^n - 1) = (2^n - 1), \\ 2\text{D} : |S(n)| &= 2 \times 2^{1n} (2^n - 1) = 2^{n+1} (2^n - 1), \\ 3\text{D} : |S(n)| &= 3 \times 2^{2n} (2^n - 1), \\ 4\text{D} : |S(n)| &= 4 \times 2^{3n} (2^n - 1) = 2^{3n+2} (2^n - 1), \\ n &\in \mathbb{N}_0. \end{aligned} \quad (13)$$

As can be seen, the count $|S(n)|$ grows exponentially. In three and higher dimensions it rapidly becomes staggering.

7. Fourier transform

It is known that the one-dimensional RPF sequence is almost periodic (*i.e.* limit quasi-periodic). Hence, its Fourier transform is of the pure point kind. Since our recursion rule is a straightforward generalization of the one-dimensional rule, the almost-periodic nature of the sequence and its corollary, the pure point Fourier spectrum, must hold also in arbitrary dimension. As an illustration of this fact we show in Fig. 11 an image of the Fourier transform of the sixth generation of the two-dimensional RPF.

8. Is there a dragon surface?

It is well known that unfolding a one-dimensional PF sequence produces a plane-filling dragon curve. Fig. 12 shows the fourth generation of the dragon curve, that is, its segment produced by unfolding a four times folded sheet of paper. It is natural to ask whether this generalizes to higher dimensions, that is, whether there is a dragon (hyper-)surface. Unfortunately, the straightforward simple answer is negative. However, the situation is more subtle and interesting.

Let us recall that the folds in any dimension are labelled by the coordinate axis perpendicular to them.

Consider a two-dimensional RPF structure. Cut it up into strips along the horizontal (alias 2 or y) folds. Each strip contains a one-dimensional PF sequence of vertical (alias 1 or x) folds. Thus, upon unfolding it will produce a dragon strip. The trouble is that adjacent strips do not match up. Starting at adjacent folds the strips diverge; this is shown in Fig. 13. Upon completion the dragon strip eventually forms a square honeycomb. Its walls are square facets parallel to the 12 (xy)

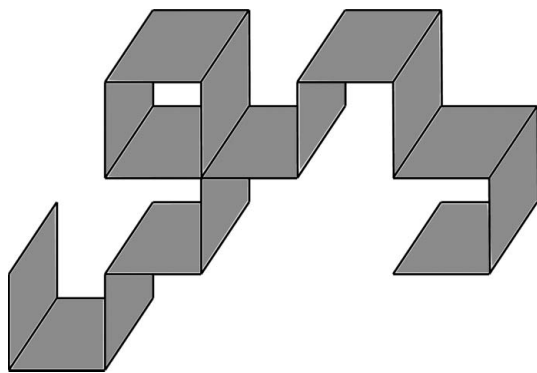


Figure 12
Fourth generation segment of the dragon curve.

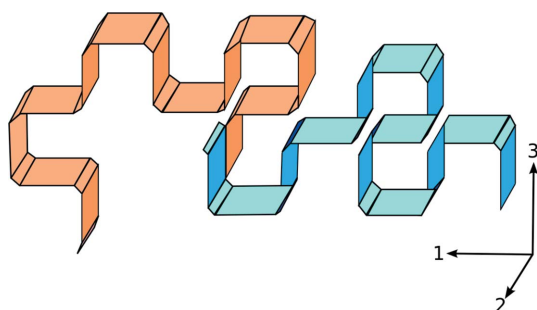


Figure 13
Segments of two adjacent folded and unfolded strips. The strips do not match up: starting at adjacent folds they diverge. The structure is open in the 2 direction; the (31) facets are missing.

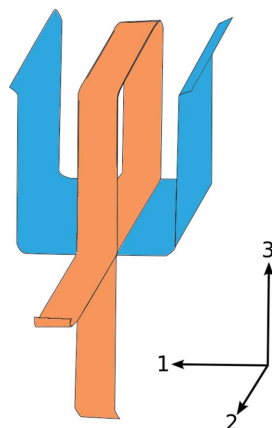


Figure 14
A segment of the two intertwined honeycombs. For clarity, only a narrow strip of the y honeycomb (orange) is shown.

and 23 (yz) planes. It is open in the 2 (y) direction; in other words the facets parallel to the 31 (zx) plane are missing as shown in Fig. 13. Alternatively, one may view the square honeycomb as a cylinder segment with the dragon curve as its directrix and the vertical segment as its generatrix.

The union of all square honeycombs may be considered to be the space-filling dragon surface. Here one may take one of two viewpoints. One may ignore the misfits of adjacent dragon strips and simply match up the complete honeycombs. It is,

however, preferable to consider the dragon curves with rounded corners and accept that the resulting dragon surface is discontinuous.

The preceding consideration must be repeated with vertical strips, that is interchanging $1 \leftrightarrow 2$ ($x \leftrightarrow y$). That leads to the conclusion that the two honeycombs are intertwined; thus the resulting dragon surface eventually cuts up three dimensions into an infinite ‘crystalline’ array of cubic cells while the 12 (xy) facets are covered twice, as shown in Fig. 14.

In general, for a d -dimensional PF structure the dragon hypersurface will cut up the $(d + 1)$ -dimensional embedding space into an infinite ‘crystalline’ array of hypercubic cells with multiple covering of a subset of facets.

9. Conclusion and outlook

We have generalized the recursion rule for the one-dimensional RPF sequence to arbitrary dimension. As an illustrative example we have explicitly constructed the two-dimensional version of the RPF structure. We have computed its rectangle complexity, that is, the symbolic complexity referred to rectangles. We have shown that the PF structures readily yield interesting novel ‘paperfolding’ tilings. We have also discussed possible generalizations of the dragon curve and the difficulties thereof.

There remain quite a few challenges:

- (i) To find and prove an analytic formula for the rectangle complexity, or, at least, for the line complexity of the two-dimensional RPF.
- (ii) An even harder task would be to find a formula valid for higher dimensions.
- (iii) Compute the symbolic complexity referred to lattice animals (polyominoes) and find the respective formula.
- (iv) Construct multidimensional generalized (*i.e.* not regular) PF structures and compute their complexities.

References

Allouche, J.-P. (1992). *Bull. Aust. Math. Soc.* **46**, 23–32.
 Allouche, J.-P. & Shallit, J. (2003). *Automatic Sequences: Theory, Applications, Generalizations*. Cambridge University Press.
 Barbé, A. & von Haeseler, F. (2004). *J. Phys. A Math. Gen.* **37**, 10879–10898.
 Barbé, A. & von Haeseler, F. (2005). *J. Phys. A Math. Gen.* **38**, 2599–2622.
 Barbé, A. & von Haeseler, F. (2007). *Int. J. Bifurcation Chaos*, **17**, 1265–1303.
 Ben-Abraham, S. I. & Quandt, A. (2011). *Philos. Mag.* **91**, 2718–2727.
 Davis, C. & Knuth, D. E. (1970a). *J. Recreational Math.* **3**, 66–81.
 Davis, C. & Knuth, D. E. (1970b). *J. Recreational Math.* **3**, 133–149.
 Dekking, M. (2012). *Theor. Comput. Sci.* **414**, 20–37.
 Dekking, M., Mendès-France, M. & van der Poorten, A. J. (1982a). *Math. Intelligencer*, **4**, 130–138.
 Dekking, M., Mendès-France, M. & van der Poorten, A. J. (1982b). *Math. Intelligencer*, **4**, 173–181.
 Dekking, M., Mendès-France, M. & van der Poorten, A. J. (1982c). *Math. Intelligencer*, **4**, 190–195.
 Gardner, M. (1967a). *Sci. Am.* **216**, 124–129.
 Gardner, M. (1967b). *Sci. Am.* **216**, 116–123.

- Gardner, M. (1967*c*). *Sci. Am.* **217**, 112–116.
- Genet, C. K. & Ebbesen, T. W. (2007). *Nature (London)*, **445**, 39–46.
- Grünbaum, B. & Shephard, G. C. (1986). *Tilings and Patterns*. New York: W. H. Freeman and Company.
- Julien, A. (2009). Thesis. Université Claude Bernard Lyon 1, France.
- Julien, A. (2010). *Ergodic Theory Dyn. Systems*, **30**, 489–523.
- Robinson, R. M. (1971). *Inventiones Math.* **12**, 177–209.
- Salon, O. (1989). *J. Théorie Nombres Bordeaux*, **1**, 1–26.